Detection of subsurface meltwater in East Antarctica using SAR Interferometry

MSc Geomatics Graduation Plan

Weiran Li

Graduation Committee

Main Mentor:
Agung Indrajit, MSc
OTB, Faculty of Architecture, TU Delft
Specialisation: Interferometry SAR, Polarimetry SAR, Object Oriented Classification, Hyper-Spectral Analysis; Geostatistics, 3D Analysis, Data Visualization, Geodatabase; Geodynamics Application, CORS Services

Second Mentor(s):
Dr. J. F. (Paco) López-Dekker
Geoscience and Remote Sensing, Faculty of Civil Engineering and Geosciences, TU Delft
Specialisation: Synthetic Aperture Radar (SAR), Bistatic SAR, Interferometry

Dr. S. L. M. (Stef) Lhermitte
Geoscience and Remote Sensing, Faculty of Civil Engineering and Geosciences, TU Delft
Specialisation: Remote sensing; specifically in the use of multi-source remote sensing and land surface modelling to assess cryosphere, atmosphere and ecosystem dynamics

1 Introduction

As the largest ice body on Earth, the Antarctic Ice Sheet contains an ice volume of 27 million km^3, equivalent to $58m$ potential sea-level rise (Fretwell *et al.*, 2013). It has a significant impact on global climate circulation (Tedesco, 2009). 74% of its coastline is surrounded by ice shelves, the extensions of land ice floating in the ocean (Bindschadler *et al.*, 2011). These ice shelves play an important role in controlling the stability and regulating mass balance of the ice sheet via the buttressing effect (Dupont and Alley, 2005; Rignot *et al.*, 2013). The loss of these ice shelves may lead to a considerable discharge of the grounded ice (Rignot *et al.*, 2004). For this reason, attention has been drawn to observing the evolvement of the Antarctic ice shelves, in order to assess the status and change of the Antarctica Ice Sheet and its impact on a global scale.

In recent decades, multiple ice-shelf collapses have been observed in Antarctica, among which Larsen A (1995) and Larsen B (2002) are documented and related to surface meltwater (Banwell, MacAyeal and Sergienko, 2013). Although the cause of the recent calving event of Larsen C (2017) remains unknown, the mechanism of water melting and ponding has been proposed as a possibility (Hogg and Hilmar Gudmundsson, 2017). Meltwater that leads to these abrupt ice-shelf losses has the characteristic of being intense, extensive or prolonged (Luckman *et al.*, 2014). Meltwater on surface or subsurface usually percolates into the firn layer, an intermediate between snow and ice, where it refreezes into ice due to a lower temperature, densifying the firn, saturating it, and releasing heat to the layer (Ligtenberg, 2014; Luckman *et al.*, 2014). Once the water cannot be accommodated, it may form ponds, and eventually drain towards the ocean (Ligtenberg, 2014). The drainage exerts tensile flexture stresses, and results in a collapse in the ice sheet (MacAyeal and Sergienko, 2013). Therefore, careful observations and thorough studies on the meltwater phenomenon are of great importance.

While the above process has been frequently recognised in Greenland and the Antarctic Peninsula, the surface mass in East Antarctica has been generally assumed to be stable. However, a recent research (Lenaerts *et al.*, 2016) revealed the existence of well-formed meltwater streams and storage on Roi Baudouin Ice Shelf (RBIS), Dronning Maud Land, East Antarctica. Among these findings, multiple meltwater features are in the form of subsurface lakes, which is unprecedented in East Antarctica. One of the lakes reported is located about four metres under the surface, with the depth of several metres, and a diameter of approximately one kilometre. This finding indicates a potential vulnerability of East Antarctica in the following perspectives: i) as is mentioned above, the englacial refreezing process of meltwater transmits heat, enters the sub-shelf cavity and enhances basal melting rates, and ii) future climate change may give rise to water drainage in this area, causing the similar collapse as the ice-shelf calving events that have happened in the Antarctic Peninsula (Lhermitte, 2017).

Compared to the existence of surface meltwater in East Antarctica that has been reported and observed in a previous research (Langley *et al.*, 2016), the knowledge of the subsurface melt features is limited. Currently, they have been pinpointed by the *in situ* observation and measurement using ground-penetrating airborne radar (Lenaerts *et al.*, 2016). Their locations and geometric properties have been estimated. But to gain a comprehensive understanding of the subsurface melting taking place in East Antarctica, or more specifically on RBIS, more information on its spatial and temporal development is needed, and the acquisition requires a proper tool.

The remote location of East Antarctica limits continuous *in situ* observation, the cloud cover and polar night restrict the measurement using passive remote sensing systems, resulting in insufficient satellite images (Luckman *et al.*, 2014; Langley *et al.*, 2016), and the requirement for sufficient ground-ice penetration depth sets limitation to short-wavelength measurements. It is also ideal to have a relatively high spatial and temporal resolution. Over the past years, a number of researches with the purpose of observing and monitoring the ice sheet adopting Synthetic Aperture Radar (SAR) have been carried out in Greenland (Johansson and Brown, 2012; Miles *et al.*, 2017), where the limitations are similar to Antarctica. With the advantage and potential shown in these projects, the use of Sentinel-1 has been recommended (Johansson and Brown, 2012; Luckman *et al.*, 2014).

Sentinel-1 is within the frame of the Global Monitoring for Environment and Security (GMES) Space Component programme undertaken by the European Space Agency (ESA) (Torres *et al.*, 2012). It applies C-band, which has a penetration ability of several metres, theoretically sufficient in this specific case (Miles *et al.*, 2017). The coverage of the S-1 system is considerably wide, with up to $250km$ under Interferomatric Wide Swath Mode, and the spatial resolution is moderate (Torres *et al.*, 2012; Yague-Martinez *et al.*, 2016). Its constellation involves two polar-orbiting satellites, each with a 12-day revisit time (Torres *at al.*, 2012). And in the acquired images, both amplitude and phase information are preserved. This mechanism enables change detection as well as volume measurement in principle, which is expected to facilitate the observation of the subsurface lakes.

2 Related work

Although the research of Lenaerts *et al.* (2016) is the first time that such subsurface water features have been found on East Antarctica, the same phenomenon has been observed in Greenland Ice Sheet (GrIS) and several ice shelves in West Antarctica (Hubbard *et al.*, 2016) and different remote sensing instruments have been used for the observation. Koenig *et al.* (2015) applied airborne radar in ultra-wideband to detect the ice-water interface based on the difference between the dielectric constant of the two media. Supportive visible imagery was also used to examine surface features that indicate the presence of the meltwater underneath.

Another research to monitor surface and subsurface lakes on the GrIS (Miles *et al.*, 2017) applied Sentinel-1 in combination with Landsat-8 OLI imagery. Regarding the application of Sentinel-1, the data used was Level-1 images in the category of Ground-Range Detected (GRD) product from the Extra-Wide swath (EW) acquisition. This type of data have a broad coverage with medium spatial resolution, lack phase information, and are georeferenced and time-tagged (The European Space Agency [ESA], n.d.). Dual-polarisation images (HH and HV) were used to compensate for each other. Based on the characteristics of the data, only the magnitude of the images was analysed, therefore the areas of low backscatter, *i.e.* appearing dark in the Sentinel-1 imagery, and invisible in the Landsat imagery, were directly defined as subsurface lakes (Miles *et al.*, 2017).

The above-mentioned two methods are compared in Miles *et al.* (2017). The advantage of the method in Koenig *et al.* (2015) is that the lake depth could be determined because of the sufficient L-band penetration. But the spatial and temporal coverage of the radar restrains the areal measurement and observation during winter. The Sentinel-1 EW GRD measurement compensates for that. There is a discrepancy between the time of presence of different researches, and it could be caused by the difference in penetration depths.

With respect to our region of interest (Lenaerts *et al.*, 2016), ground penetrating radar was adopted for depth measurement. By observing the radar cross-section, the upper and lower boundary of the subsurface could be recognised. However, it has the same restrictions as the ones in Koenig *et al.* (2015).

The studies using SAR Interferometry (InSAR) were usually carried out with the aim of mapping glacier surface displacement. Conservatively, by analysing the phase coherence in the interferogram generated by two images taken for the same area at different time, the terrain motion can be retrieved (Weber Hoen and Zebker, 2000). However, in the ice-covered area, a great amount of phase decorrelation can be caused by volume scatter, and this feature is used by Weber Hoen and Zebker (2000) to determine penetration depths of InSAR, as well as by Banda *et al.* (2013) to analyse subsurface ice structure. Based on these ideas, this project will be carried out with the advantage of Sentinel-1 Single Look Complex (SLC) products, which preserve both amplitude and phase information, in order to explore and apply the potential of InSAR in subsurface water observation.

3 Research objectives

With the background and related work introduced above, it would be ideal to be able to observe the subsurface meltwater on the RBIS in East Antarctica. But the first step of this topic, is to detect these

features. The research questions are thus specified as follows:

To what extent is InSAR capable of detecting subsurface meltwater on the Roi Baudouin Ice Shelf?

To answer this, the following sub-questions are to be covered:

- How is the penetration performance of Sentinel-1 in the ice- and snow-covered area?
- How to generate the SAR interferogram best suited for subsurface water detection?
- How to determine the subsurface lakes with the information obtained and processed from Sentinel-1 data?
- Is there a temporal variation in the information obtained and processed from Sentinel-1 data?
- How does the outcome fit the ground truth?
- How does the InSAR technique perform in comparison to other orbiting remote-sensing systems?

4 Methodology

This project focuses on the processing of InSAR data, mainly using Delft Object-oriented Radar Interferometric Software (DORIS) and Python 3.4. QGIS and MATLAB may be needed for data visualisation. This chapter elaborates the work flow.

4.1 SAR Interferometry

The basic components of an InSAR image are amplitude and phase. For each pixel, the signal of it can be expressed as

$$z = \sum_{k=1}^{N} A_k e^{j\phi_k}$$

where A_k refers to the amplitude and ϕ_k is the phase of each individual scatterer. This could also be expressed in the complex form (Oost, 2016)

$$z = x + jy$$

In the InSAR signal, the amplitude represents the strength of the reflected signal, and the phase is the recorded fraction of a complete wave cycle (SkyGeo, n.d.). Both types of information are needed for this research.

The reflection depends on surface roughness, incidence angle and dieletric property. For a region covered by snow, ice and potential water, this means that the different facies can be roughly distinguished by the amplitude of the recorded signal in an InSAR image. Miles *et al.* (2017) detected the subsurface lakes with amplitude information, defining them as small, dark areas appearing in Sentinel-1 GRD imagery.

The previous studies mainly focus on the different behaviours of water, ice and snow when interacting with microwave, which are expected to be reflected in amplitude of the Sentinel-1 imagery. Fresh snow is expected to be invisible at microwave wavelengths, and firn would be distinct as well for the volume scatterers. Smooth water surface should give a low backscatter and a frozen pond shows smooth surface scatterers (Luckman *et al.*, 2014). This should be obvious in locating the subsurface lakes and measuring the width.

The coherence between InSAR images depends on a series of factors including perpendicular baseline, surface movements, and volume (Weber Hoen and Zebker, 2000). Therefore, attention should be paid to areas with low coherence. Once a low coherence is found, the surface features in that area such as surface melting and ice movement should be analysed first. If no or few surface factors are found, the

area is suspected to have subsurface water features.

The coherence is found by using two images, which are referred to as master and slave images respectively. The aforementioned coherence is found by coregistering the slave image with respect to the master image by estimating the offsets between them. Meanwhile, an interferogram can be formed by (De Zan, Zonno and López-Dekker, 2015)

$$I_{12} = |I_{12}|exp(j\varphi_{12}) = \overline{i_1 i_2^*}$$

and with two slave images and a master image, the phase closure is derived from the interferograms as

$$\Phi_{123} = \phi_{12} + \phi_{23} + \phi_{31}$$

and is expected to be zero. If it is not the case in the imagery, it could be presumed that the microwave has been influenced by volume scattering. In combination, these features of the InSAR information should be able to indicate the appearance of the subsurface water features.

4.2 Study region and data acquisition

The meltwater features were found on the RBIS, therefore the region of interest is mainly defined as this ice shelf. And the Sentinel-1 data are available on Copernicus Open Access Hub (Copernicus, 2017). To apply InSAR processing, the SLC products are needed, and data from two acquisition modes are available in this region: EW dual-polarisation (HH and HV) products and Interferometric Wide swath (IW) single-polarisation (HH) products. However, as will be mentioned in sub-section 4.3, only the latter products will be used. They appear on the map as in Figure 1.

In Figure 1, the IW data are obtained by ascending track 15, ascending track 59, ascending track 74 and descending track 136. But there are still limitations to these data. Optimally, Sentinel-1 data are expected to have a 6-day revisit time, with both Sentinel-1A and Sentinel-1B functioning. In this region, however, the products only come from Sentinel-1A, which results in a relatively low temporal resolution of 12 days theoretically. Since the environment in Antarctica is highly dynamic, a longer revisit time will lead to less coherence, and it will be hard to interpret the image. Therefore, a requirement is set that data with a revisit time longer than 12 days should not be considered. This excludes descending track 136 from data processing, as it has a revisit time of 24 days.

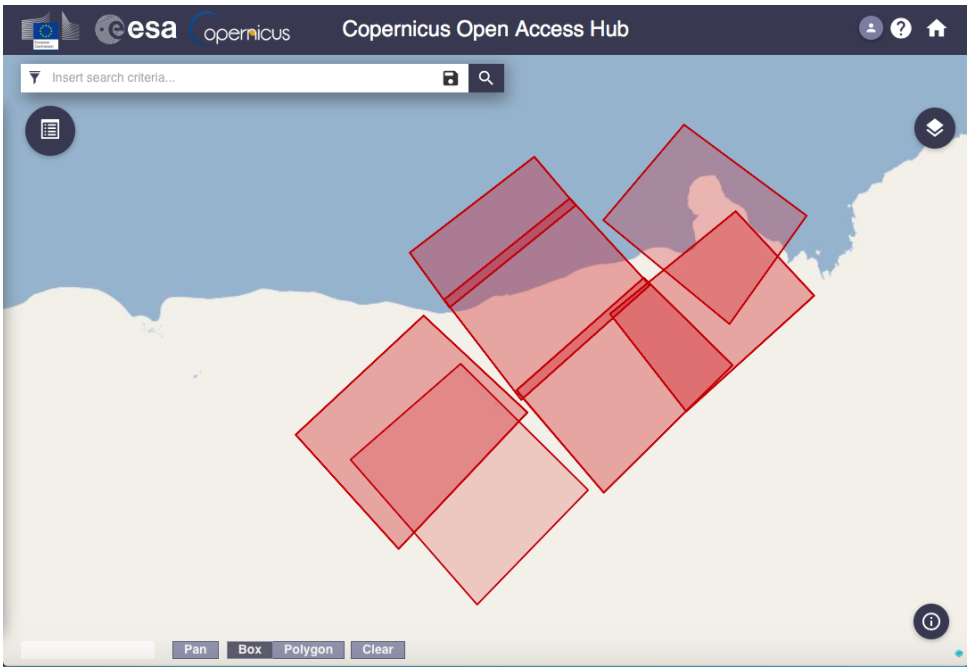

Figure 1: Copernicus Open Access Hub search results

On the other hand, the selection is based on the intersection between the images and the bounding box of the region of interest, instead of the exact shape of the region. The actual intersection is shown in Figure 2. In this figure, the yellow feature is the region of interest, green represents ascending track 15, ocher ascending track 59, purple ascending track 74 and cyan descending track 136. Obviously there is no overlap between the region of interest and the ascending track 74, so this set of data also will not be used.

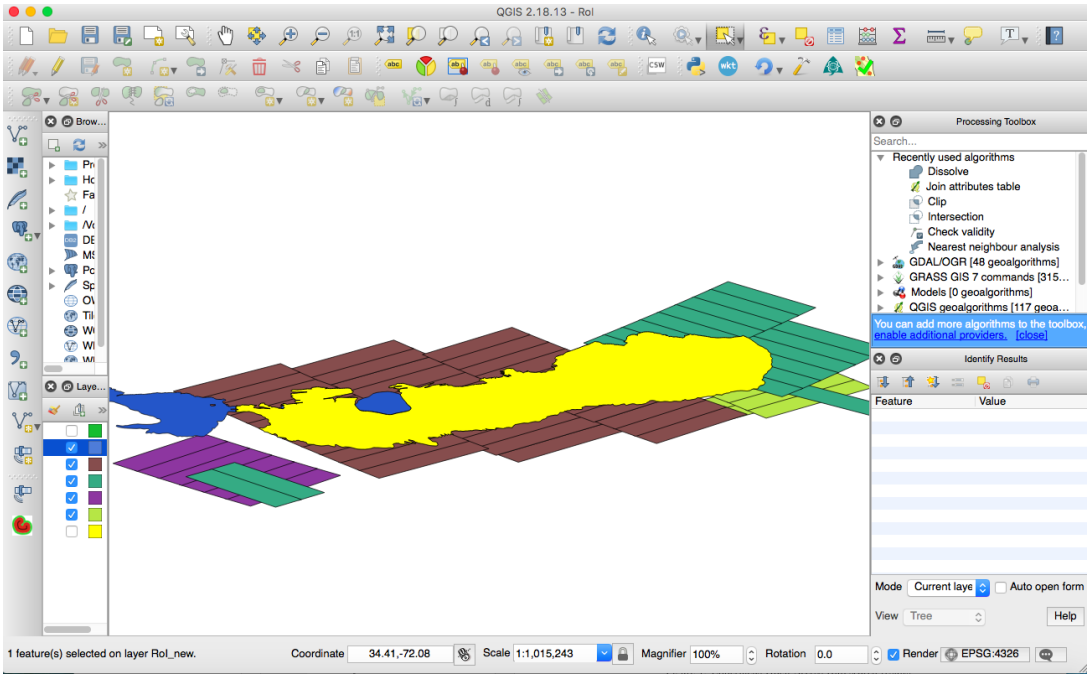

Figure 2: Coverage of the images in shapefiles, processed by DORIS and visualised by QGIS

4.3 InSAR processing

This project chooses DORIS 5 for InSAR processing, because it automatically processes the data stacks from downloading to forming interferometric products via coregistration with orbit information. But this is usually not accurate enough, so further processing is needed (Oost, 2016).

The output from DORIS, including the ground range and azimuth resolution, orbit information, reference phase, and geocode *etc.* are then used for offset tracking, in order to reduce the influence from the surface, and to better reveal the subsurface features. This is realised via cross-correlation. The cross-correlation includes coherent (CCC) and incoherent (ICC) methods, which refer to using both amplitude and phase information, and using only amplitude information, respectively. The previous studies (De Zan, 2014; Oost, 2016) suggest that although CCC has a theoretically better accuracy than ICC, it has a higher demand for the stability of the phase signal, therefore ICC is more reliable. However, as the comparison is within the scope of this project, both methods will be tested to find an optimal method to obtain the amplitude, coherence, interferogram and closure information in the region of interest.

4.4 Ground truth

Apart from InSAR technique, the ground truth also takes part in this project. Measurements will be carried out along the ice shelf by the research team of Lanaerts *et al.*, and they will be categorised into two groups. One will be combined with the InSAR images, providing the actual characteristics of the subsurface lakes. Because it is likely that very low coherence appear in this area, and the cause for this varies, it is important to have the reference of what is actually happening, including wind, snow, surface melt and subsurface water features. The other group is used as validation group for the aforementioned detection method.

4.5 Performance analysis

As is mentioned in subsection 4.4, the validation will be performed with some of the ground truth data. The result can also be compared with other orbit remote sensing methods, such as L-band SAR and Landsat-8.

5 Time planning

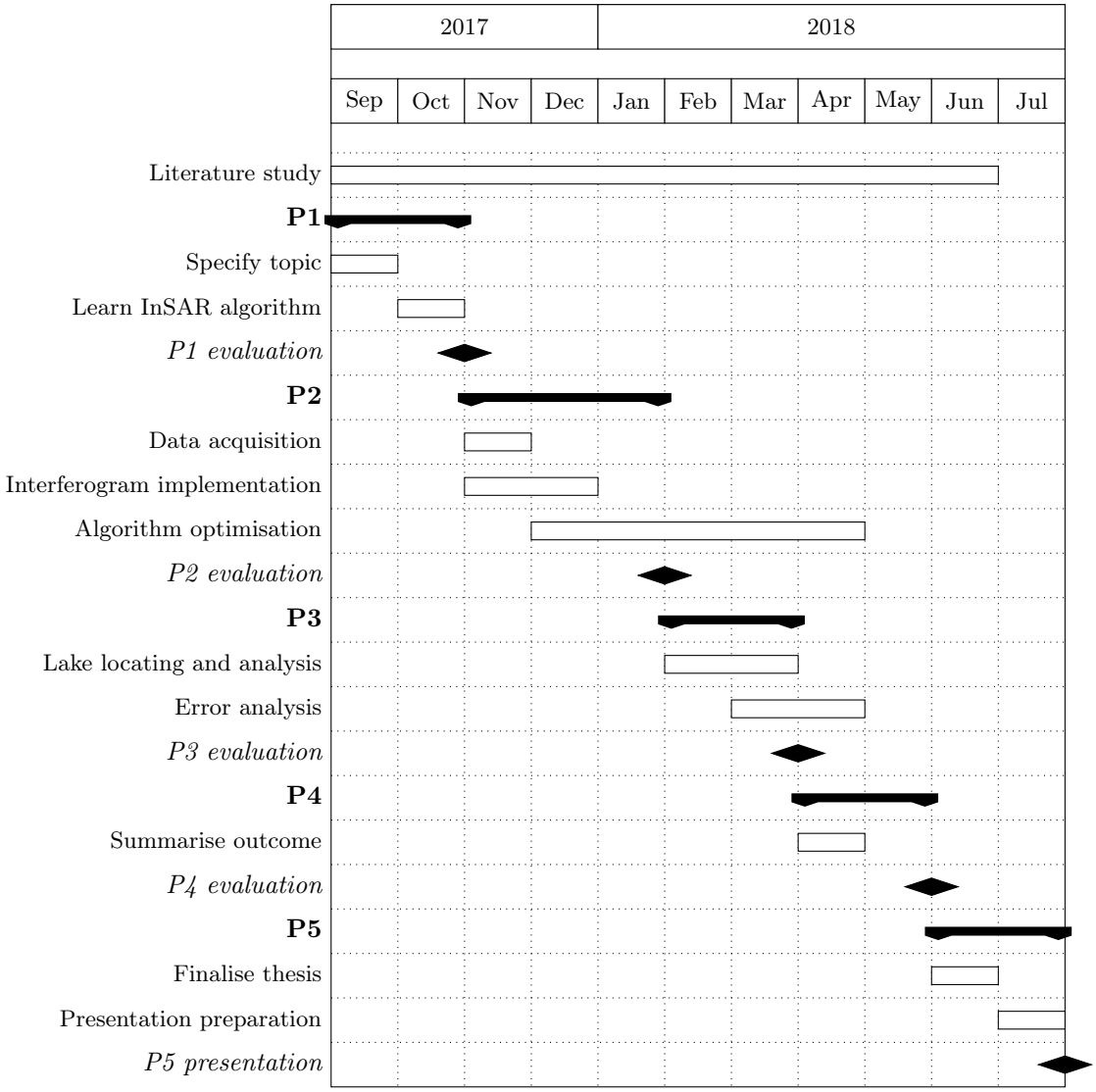

Figure 3: Project timeline

Reference

Banda, F., Dall, J., Tebaldini, S., and Rocca, F. (2013) Tomographic SAR Analysis of Subsurface Ice Structure in Greenland: First Results. In: *Geoscience and Remote Sensing Symposium (IGARSS), 2013 IEEE International*. City: Melbourne, VIC, Australia, 236-239 (doi:10.1109/IGARSS.2013.6721135).

Banwell, A. F., MacAyeal, D. R., and Sergienko, O. V. (2013) Breakup of the Larsen B Ice Shelf triggered by chain reaction drainage of supraglacial lakes. *Geophys. Res. Lett.*, 40, 5872-5876 (doi:10.1002/2013GL057694).

Beckmann, P. and Spizzichino, A. (1987) The scattering of electromagnetic waves from rough surfaces. *Norwood, MA, Artech House, Inc.*, 1987, 511.

Bindschadler, R., Choi, H., Wichlacz, A., Bingham, R., Bohlander, J., Brunt, K., Corr, H., Drews, R., Fricker, H., Hall, M., Hindmarsh, R., Kohler, J., Padman, L., Rack, W., Rotschky, G., Urbini, S., Vornberger, P., and Young, N. (2011) Getting around Antarctica: new high-resolution mappings of the grounded and freely-floating boundaries of the Antarctic ice sheet created for the International Polar Year. *Cryosphere*, 5, 569-588 (doi:10.5194/tc-5-569-2011).

Copernicus (2017) Open Access Hub. [online] Available at: `https://scihub.copernicus.eu` [Accessed 2 Nov. 2017].

De Zan, F. and Guarnieri, A. M. (2006) TOPSAR: Terrain Observation by Progressive Scans *IEEE Transactions on Geoscience and Remote Sensing*, 44(9), 2352-2360 (doi:10.1109/TGRS.2006.873853).

De Zan, F. (2014) Accuracy of incoherent Speckle Tracking for circular Gaussian Signals. *IEEE Geosci. Remote Sens- ing Lett.*, 11(1), 264âĂŞ267 (doi:10.1109/LGRS.2013.2255259).

De Zan, F., Zonno, M., and López-Dekker, P. (2015) Phase Inconsistencies and Multiple Scattering in SAR Interferometry. *IEEE Transactions on Geoscience and Remote Sensing*, 53(12), 6608-6616 (doi:10.1109/TGRS.2015.2444431).

Dupont, T.K. and Alley, R.B. (2005) Assessment of the importance of ice-shelf buyyressing to ice-sheet flow. *Geophys. Res. Lett.*, 32(4), L04503 (doi:10.1029/2004GL022024).

Fretwell, P., Pritchard, H. D., Vaughan1, D. G., Bamber, J. L., Barrand, N. E., Bell R., Bianchi, C., Bingham, R. G., Blankenship, D. D., Casassa, G., Catania, G., Callens, D., Conway, H., Cook, A. J., Corr, H. F. J, Damaske, D., Damm, V., Ferraccioli, F., Forsberg, R., Fujita, S., Gim, Y., Gogineni, P., Griggs, J. A., Hindmarsh, R. C. A., Holmlund, P., Holt, J. W., Jacobel, R. W., Jenkins, A., Jokat, W., Jordan, T., King, E. C., Kohler, J., Krabill, W., Riger-Kusk, M., Langley, K. A., Leitchenkov, G., Leuschen, C., Luyendyk, B. P., Matsuoka, K., Mouginot, J., Nitsche, F. O., Nogi, Y., Nost, O. A., Popov, S. V., Rignot, E., Rippin, D. R., Rivera, A., Roberts, J., Ross, N., Siegert, M. J., Smith, A. M., Steinhage, D., Studinger, M., Sun, B., Tinto, B. K., Welch, B. C., Wilson35, D., Young, D. A., Xiangbin, C., and Zirizzotti, A. (2013) Bedmap2: improved ice bed, surface and thickness datasets for Antarctica. *The Cryosphere*, 7, 375-393 (doi:10.5194/tc-7-375-2013).

Hogg, A. E. and Hilmar Gudmundsson, G. (2017) Impacts of the Larsen-C Ice Shelf calving event. *Nature Climate Change*, 7, 540-542. (doi:10.1038/nclimate3359).

Hubbard, B., Luckman, A., Ashmore, D. W., Bevan, S., Kulessa, B., Kuipers Munneke, P., Philippe, M., Jansen, D., Booth, A., Sevestre, H., Tison, J.-L., O'Leary, M., and Rutt, I. (2016) Massive subsurface ice formed by refreezing of ice-shelf melt ponds. *Nature Communications*, 7(11897), 1-6 (doi:10.1038/ncomms11897).

Johansson, A.M. and Brown, I.A. (2012) Observations of supra-glacial lakes in west Greenland using

winter wide swath Synthetic Aperture Radar. *Remote Sensing Letters*, 3(6), 531-539 (doi:10.1080/01431161.2011.637527).

Koenig, L. S., Lampkin, D. J., Montgomery, L., N., Hamilton, S. L., Turrin, J. B., Joseph, C. A., Moustafa, S. E., Panzer, B., Casey, K. A., Paden, J. D., Leuschen, C., and Gogineni, P. (2015) Wintertime storage of water in buried supraglacial lakes across the Greenland Ice Sheet. *The Cryosphere*, 9, 1333-1342 (doi:10.5194/tc-9-1333-2015).

Lanaerts, J. T. M., Lhermitte, S., Drews, R., Ligtenberg, S. R. M., Berger, S., Helm, V., Smeets, C. J. P. P., van den Broeke, M. R., van de Berg, W. J., van Meijgaard, E., Eijkelboom, M., Eisen, O., and Pattyn, F. (2016) Meltwater produced by wind-albedo interaction stored in an East Antarctic ice shelf. *Nature Climate Change*, 7, 58-62 (doi:10.1038/nclimate3180).

Langley, E. S., Leeson, A. A., Stokes, C. R., and Jamieson, S. S. R. (2016) Seasonal evolution of supraglacial lakes on an East Antarctic outlet glacier. *Geophys. Res. Lett.*, 43, 8563-8571 (doi:10.1002/2016GL069511).

Li, Z. and Bethel, J. (2008) Image Coregistration in SAR Interferometry. In: *The International Archives of the Phorogrammetry, Remote Sensing and Spatial Information Sciences*, 37(B1), Beijing 2008.

Ligtenberg, S. (2014) *The present and future state of the Antarctic firn layer.* PhD. Utrecht University.

Lhermitte, S. (2017) *Meltwater lakes in East Antarctic.* [online] EarthMapps.io. Available at: `http://www.benemelt.eu/` [Accessed 30 Oct. 2017].

Luckman, A., Elvidge, A., Jansen, D., Kulessa, B., Kuipers Munneke, P., King, J., and Barrand, N. E. (2014) Surface melt and ponding on Larsen C Ice Shelf and the impact of Fö winds. *Antarctic Science*, 26(6), 625-635 (doi:10.1017/S0954102014000339).

MacAyeal, D. R. and Sergienko, O. V. (2013) The flexural dynamics of melting ice shelves. *Annals of Glaciology*, 54(63), 1-10 (doi:10.3189/2013AoG63A256).

Miles, K. E., Willis, I. C., Benedek, C. L., Williamson, A. G., and Tedesco, M. (2017) Toward Monitoring Surface and Subsurface Lakes on the Greenland Ice Sheet Using Sentinel-1 SAR and Landsat-8 OLI Imagery. *Front. Earth Sci.*, 5(58), 1-17 (doi:10.3389/feart.2017.00058).

Miranda, N. (2014) Definition of the TOPS SLC deramping function for products generated by the S-1 IPF. Eur. Space Agency, Paris, France, Tech. Rep., 2014.

Oost, R. (2016) *A SAR-derived long-term record of glacier evolution in North-West Greenland.* MSc. Delft University of Technology.

QGIS Development Team (2017) QGIS (Version 2.18) [Computer programme]. Available at: `http://qgis.osgeo.org` [Accessed 30 Dec. 2017].

Rignot, E., Casassa, G., Gogineni, P., Krabill, W., Rivera, A., and Thomas R. (2004) Accelerated ice discharge from the Antarctic Peninsula following the collapse of Larsen B ice shelf. *Geophys. Res. Lett.*, 31, L18401 (doi:10.1029/2004GL020697).

Rignot, E., Jacobs, S., Mouginot, J., and Scheuchl, B. (2013) Ice-Shelf Melting Around Antarctica. *Science*, 341(6143), 266-270 (doi:10.1126/science.1235798).

SCAR Antarctic Digital Database (2016) British Antarctic Survey Geodata Portal - Antarctic Digital Database [online] Available at: `http://add.antarctica.ac.uk/repository` [Accessed 2 Nov. 2017].

Skala, W. (2013) Drawing Gantt Charts in LaTeX with Ti*k*Z. University of Salzburg.

SkyGeo (n.d.) InSAR Technical Background. [online] Available at: `https://skygeo.com/insar-technical-background/` [Accessed 27 Dec. 2017].

Tedesco, M. (2009) Assessment and development of snowmelt retrieval algorithms over Antarctica from K-band spaceborne brightness temperature (1979-2008). *Remote Sensing of Environment*, 113(5), 979-997 (doi:10.1016/j.rse.2009.01.009).

The European Space Agency (ESA) (n.d.) Products and Algorithms. [online] Sentinel Online. Available at: `https://sentinels.copernicus.eu/web/sentinel/technical-guides/sentinel-1-sar/products-algorithms` [Accessed 1 Nov. 2017].

Torres, R., Snoeij, P., Geudtner, D., Bibby, D., Davidson, M., Attema, E., Potin, P., Rommen, B., Floury, N., Brown, M., Navas Traver, I., Deghaye, P., Duesmann, B., Rosich, B., Miranda, N., Bruno, C., L'abbate, M., Croci, R., Pietropaolo, A., Huchler, M., and Rostan, F. (2012) GMES Sentinel-1 mission. *Remote Sensing of Environment*, 120, 9-24 (doi:10.1016/j.rse.2011.05.028).

TU Delft Radar Group (2017) Delft Object-oriented Radar Interferometric Software (Version 5.0) [Computer programme]. Available at: `https://github.com/TUDelftGeodesy/Doris` [Accessed 30 Dec. 2017].

Wang, T., Jónsson, S., and Hansson, R. (2011) Coregistration between SAR Image Subsets Using Pointwise Targets. *Proc. 'Fringe 2011 Workshop', Frascati, Italy*, 19-23 September 2011.

Weber Hoen, E. and Zebker, H. A. (2000) Penetration Depths Inferred from Interferometric Volume Decorrelation Observed over the Greenland Ice Sheet. *IEEE Transactions on Geoscience and Remote Sensing*, 38(6), 2571-2583 (doi:10.1109/36.885204).

Yague-Martinez, N., Rodriguez Gonzalez, F., Balss, U., Breit, H., and Fritz, T. (2014) TerraSAR-X TOPS, ScanSAR and WideScanSAR interferometric processing. In *Proc. 10th EUSAR*, Jun. 2014, 1-4.

Yague-Martinez, N., Prats-Iraola, P., Rodriguez Gonzalez, F., Brcic, R., Shau, R., Geudtner, D., Eineder, M., and Bamler, R. (2016) Interferometric Processing of Sentinel-1 TOPS Data. *IEEE Transactions on Geoscience and Remote Sensing*, 54(4), 2220-2234 (doi:10.1109/TGRS.2015.2497902).